


## Article

# The Roughness Effect on the Preparation of Durable Superhydrophobic Silver-Coated Copper Foam for Efficient Oil/Water Separation

Aikaterini Baxevani, Fani Stergioudi \*  and Stefanos Skolianos

Physical Metallurgy Laboratory, School of Mechanical Engineering, Aristotle University of Thessaloniki, GR-54124 Thessaloniki, Greece; ampaxeva@meng.auth.gr (A.B.); skol@meng.auth.gr (S.S.)

\* Correspondence: fstergio@auth.gr

**Abstract:** In recent decades, there has been a significant interest in superhydrophobic coatings owing to their exceptional properties. In this research work, a superhydrophobic coating was developed on copper foams with a different roughness via immersion in  $\text{AgNO}_3$  and stearic acid solutions. The resulting foams exhibited water contact angles of  $180^\circ$ . Notably, surface roughness of the substrate influenced the development of silver dendrites and stearic acid morphologies, leading to different structures on rough and smooth copper foams. Separation efficiency was maintained above 94% for various pollutants, suggesting good stability and durability, irrespective of the substrate's roughness. Conversely, absorption capacity was influenced by surface roughness of the substrate, with smooth copper foams demonstrating higher absorption values, primarily due to its uniform porosity and microstructure, which allowed for efficient retention of pollutants. Both copper foams exhibited excellent thermal and chemical stability and maintained their hydrophobic properties even after a 40 h exposure to harsh conditions. Mechanical durability of modified copper foams was tested by dragging and in ultrasounds, exhibiting promising results. The samples with the smooth substrate demonstrated improved coating stability.

**Keywords:** superhydrophobicity; copper foam; durability; stability; oil/water separation; roughness; absorption capacity



**Citation:** Baxevani, A.; Stergioudi, F.; Skolianos, S. The Roughness Effect on the Preparation of Durable Superhydrophobic Silver-Coated Copper Foam for Efficient Oil/Water Separation. *Coatings* **2023**, *13*, 1851. <https://doi.org/10.3390/coatings13111851>

Academic Editor: Alexandra Muñoz-Bonilla

Received: 22 September 2023  
Revised: 21 October 2023  
Accepted: 24 October 2023  
Published: 27 October 2023



**Copyright:** © 2023 by the authors. Licensee MDPI, Basel, Switzerland. This article is an open access article distributed under the terms and conditions of the Creative Commons Attribution (CC BY) license (<https://creativecommons.org/licenses/by/4.0/>).

## 1. Introduction

In the past few decades, there has been a notable interest in superhydrophobic coatings due to their remarkable characteristics and wide range of applications, including anti-icing, anti-fogging, self-cleaning capability and the ability to separate oil and water, which contribute significantly to their widespread usage [1–3]. Water contamination due to oil exploration, transportation, refining and effluents from various industries leads to severe environmental and economic consequences [4,5]. Conventional oil–water separation strategies including air flotation, in situ burning, oil-absorbing materials, oil skimmers, flocculation, gravity settling, centrifugation, gas flotation and electrochemical techniques suffer from limitations such as low selectivity, prolonged separation time, complex separation processes and inefficiency in large-scale applications [6–8]. Hence, it is crucial to develop a low-cost and efficient strategy to achieve complete separation of oil/water mixtures.

Taking inspiration from the exceptional water-repellent properties exhibited with natural elements like lotus leaves, desert beetles and water striders, artificial superhydrophobic surfaces have garnered significant interest [9–12]. Lotus leaves have emerged as a symbol of superhydrophobicity and self-cleaning surfaces, giving rise to what is known as the ‘lotus effect’. While several other plants boast superhydrophobic surfaces with nearly identical contact angles, the lotus stands out for its superior stability and the impeccable quality of its water-repellent properties. This exceptional performance is attributed to the unique shape and density of the papillae, which result in an exceptionally reduced

contact area between the leaf surface and water droplets [10,13,14]. The wettability of a solid surface is influenced by two crucial factors: surface chemical compositions and micro-nanostructures [15,16]. Over time, various methods have been developed to prepare superhydrophobic materials including hydrothermal techniques, chemical etching, electrochemical deposition, the sol-gel method, spray coating, self-assembly and laser etching [15–18]. These preparation approaches primarily rely on these strategies: roughening hydrophobic surfaces and modifying rough surfaces with substances possessing low surface energy. The development of a straightforward, one-step technology for acquiring high-performance and stable superhydrophobic materials is immensely desirable [19,20].

In recent years, there has been significant interest in three-dimensional (3D) porous materials, such as organic sponges, metallic foams as well as aerogels, which offer large specific surface areas plus porosity and are considered ideal substrates for developing super-wettability materials for water/oil separation [21–24]. Copper foam is a favorable choice as a substrate for oil/water separation since it is highly amenable to various surface modifications and treatments, owing to its electrical conductivity, which allows for the integration of various functional coatings and nanomaterials. Moreover, copper foam is known for its mechanical robustness. It can withstand the handling and manipulation required during the fabrication process and can maintain its structural integrity in practical applications. Additionally, copper foams are widely available and relatively affordable, which can contribute to cost-effective fabrication methods for oil/water separation materials.

To achieve superhydrophobicity, the surface of the copper foam can be micro/nanostructured and then modified using thiols or silanes or fatty acids. This can be achieved using several methods such as chemical etching, laser ablation or chemical treatments. Xin et al. [25] created superhydrophobic and superhydrophilic sides on copper foam using laser ablation and chemical modification, involving 1H,1H,2H,2H-perfluorodecyltriethoxysilane (FAS) and graphene oxide. Zhang et al. [26] created a surface layer of HKUST-1, which was grown in situ on the copper foam and then modified with 1-Hexadecanethiol, resulting in superhydrophobicity. Song et al. [27] created superhydrophobic copper meshes by immersing them in an  $\text{AgNO}_3$  solution, followed by 1-dodecanethiol immersion, which formed a superhydrophobic surface on the copper. Zhang et al. [28] adopted a procedure that involved chemical etching in  $\text{FeCl}_3/\text{HCl}$  solutions to create rough structures on copper foam and subsequent modification with four sulfhydryl compounds to lower surface energies. In Xu et al.'s study [29], copper foams were cleaned and immersed in an ethanolic stearic acid solution to create superhydrophobic surfaces. Zhou et al. [30] employed a process involving dopamine,  $\text{AgNO}_3$  reduction and n-dodecyl mercaptan to create superhydrophobic copper foam. In Chen et al.'s study [31], copper foam was anodized in  $\text{NaOH}$ , modified with APTES and carbon nanotubes (CNTs) and immersed in silanes to achieve superhydrophobicity.

Hydrophobic nanoparticles or nanostructures incorporated into the coating that can create a rough surface structure, to increase water repellency, are also reported in the literature. Gao et al. [32] electrodeposited  $\text{CeO}_2$  nanostructures on copper foam, followed by immersion in an n-dodecyl mercaptan solution to achieve superhydrophobicity. Li et al. [33] fabricated superhydrophobic surfaces by growing  $\text{Cu}(\text{OH})_2$  nanowires and  $\text{CuS}$  nanostructures on copper foam using electrodeposition, followed by chemical modification. Zhu et al. [34] created superhydrophobic copper foams coated with various patterned nanostructures, including  $\text{Cu}(\text{OH})_2$  nanoneedles,  $\text{ZnO}$  nanocones and  $\text{ZnO}$  nanorods. In Rong et al.'s study [35], copper foam was immersed in a mixed solution containing  $(\text{NH}_4)_2\text{S}_2\text{O}_8$  and  $\text{Na}_2\text{HPO}_4$ , resulting in the growth of  $\text{Cu}_3(\text{PO}_4)_2 \cdot \text{H}_2\text{O}$  nanosheets on the surface. In Zhu et al.'s study [36], copper foams were coated with a composite material through a spray-on method using hydroxyl-functionalized multi-wall carbon nanotubes and water-based melamine formaldehyde. More complicated methods such as in Liu et al.'s study [37], who constructed superhydrophobic Janus separation materials using commercially available copper foam and silane agents through a controlled hydrophobic molecular vapor deposition process, are also reported.

The provided techniques for creating superhydrophobic copper foams indeed show promise for separating water and oil mixtures. However, there are some disadvantages that need to be addressed. Many of these techniques involve multiple steps and processes, which can be time-consuming. Some methods require specialized equipment, which may not be readily available or cost-effective for widespread adoption. The utilization of expensive materials or reagents is also an essential consideration for practical applications. Most importantly, there is a lack of understanding of interaction mechanisms.

Though there is an abundance of research related to the properties of hydrophobic coatings, when applied to surfaces, a notable void in the literature pertains to hydrophobic metal foams. As mentioned, there is a need for a better understanding of the interaction mechanisms on superhydrophobic copper foams. Additionally, the majority of studies focus on the roughness of the coating and its impact on hydrophobicity. Nonetheless, there exists a noticeable dearth of the literature concerning substrate roughness and its influence on the morphology of the hydrophobic coating.

In this research work, the alteration of the superhydrophobic coating's structure was thoroughly investigated, focusing solely on variations in the substrate's roughness. The production process of the superhydrophobic coating remains identical and is extensively detailed in our previous work [38]. Another crucial aspect examined was the mechanical resilience of the developed hydrophobic coatings. Numerous research studies are related to the growth of superhydrophobic coatings, but the lack of mechanical durability along with satisfying chemical and thermal stability hinder their widespread application.

In this research work, an effective superhydrophobic coating was successfully developed on copper foams with varying degrees of roughness, via immersion in  $\text{AgNO}_3$  and stearic acid solutions. Silver nitrate displays a swift reaction with copper and even a small amount is sufficient to adequately coat the surface. Consequently, the overlay process was simple, fast and cost-effective. Silver nitrate was employed to enhance the surface micro-roughness, a pivotal element in hydrophobic coating fabrication [39,40]. In addition, fatty acids like stearic acid, palmitic acid, lauric acid and oleic acid are renowned for their capacity to form coordinating bonds with metal nanoparticles and thus for improving the performance of superhydrophobic materials [41]. To test the coating's chemical and thermal stability, contact angle measurements were conducted after its exposure in low and high temperatures as well as in acidic and alkaline aqueous mixtures. To assess the mechanical resilience of the altered copper foams, samples were subjected to abrasion with 600-grit SiC paper with various weights on them. Samples also underwent ultrasonic treatment and retained their hydrophobic properties. In terms of absorption capacity, the superhydrophobic copper foams with a smooth substrate exhibited a greater ability to absorb. Separation efficiency remained above 94% for a range of contaminants after 10 separation cycles, with both samples indicating excellent stability and durability. The durability of the superhydrophobic copper foam, as well as the cost-effectiveness of the chosen materials and processes, should be considered as an asset in potential use in filtration applications.

## 2. Materials and Methods

### 2.1. Materials

Silver nitrate was obtained from Panreac (Barcelona, Spain) and stearic acid ( $\text{C}_{18}\text{H}_{36}\text{O}_2$ ) was a product of Merck (Darmstadt, Germany). Rough copper metal foams were provided by Metafoam Technologies (Brossard, Canada) and smooth copper foams were purchased from Hui Rui Siwang (Hengshui City, China). Both copper foams have 94% porosity and are in the form of  $10\text{ cm} \times 10\text{ cm} \times 1.6\text{ mm}$  sheets. Ethanol was purchased from Central-chem (Bratislava, Slovakia). Sodium hydroxide (NaOH) and hydrochloric acid (HCl), used in chemical stability tests, are products of Honeywell (Seelze, Germany) and Panreac (Barcelona, Spain), respectively.

## 2.2. Preparation of Superhydrophobic Copper Foam

Copper foam sheets with different struts' roughness (rough and smooth), measuring 15 mm × 15 mm × 1.6 mm, underwent ultrasonic cleaning using acetone and anhydrous ethanol. Smooth and rough substrates were produced via electrodeposition and sintering methods, respectively. Pretreated copper foam samples were submerged in a 20 mm ethanolic solution of silver nitrate (AgNO<sub>3</sub>) at 50 °C for 20 min to enhance the micro/nanoroughness of the foams. Subsequently, they were immersed in a 15 mm ethanolic solution of stearic acid for 50 min to reduce surface energy. The optimum parameters were found and analyzed in previous research work [38]. The achieved water contact angle (WCA) of the modified copper foams was 180°.

## 2.3. Characterization and Testing

Surface morphology of the superhydrophobic copper foams and substrates' roughness measurements were examined through a scanning electron microscope (Phenom ProX desktop SEM, Thermo Fisher Scientific, Eindhoven, The Netherlands). The microstructure and phases formed on superhydrophobic films were characterized using an energy dispersive spectrometer (EDS). The foam substrates' roughness measurements were examined through 3D EDS Tomography, which is a technique of a scanning electron microscope (Phenom ProX desktop SEM, Thermo Fisher Scientific). Static water contact angle measurements were conducted to evaluate wettability. Specifically, 8 µL water droplets were deposited onto the surfaces under examination in standard ambient conditions. A laboratory incubator was used for the thermal treatment of the coated samples (CLIMACELL incubator, MMM Group, Munich, Germany). Oil viscosities were measured using a rheometer (TA Discovery Hybrid Rheometer HR30). The calculation of the separation efficiency (s) involves dividing the weight of oil collected in the filtrate tank after separation ( $m_1$ ) by the weight of oil added before separation ( $m_0$ ). Separation efficiency was calculated as follows (Equation (1)):

$$\text{Separation efficiency} = \frac{m_1}{m_0} \times 100\% \quad (1)$$

Absorption capacity was calculated through Equation (2):

$$\text{Absorption capacity} = \frac{W_1 - W_2}{W_1} \quad (2)$$

where  $W_1$  is the weight of the foam before the absorption and  $W_2$  is the weight of the foam after the absorption.

## 3. Results and Discussion

### 3.1. Analysis of the Developed Morphologies on Coated Copper Foams

Surface roughness plays a crucial role in the shape of developed structures. Observed morphologies of silver dendrites, in this research work, can be divided into two categories: tree- and moss-like on rough and smooth copper foam, respectively [42,43]. Figure 1a,b show a schematic illustration of these morphologies. Figure 1c,d depict the mean value of roughness of the surface irregularities for rough and smooth copper foams, respectively. At least 10 measurements were conducted with each sample.  $R_z$  represents the mean magnitude of the heights of the five highest peaks and the depths of the five deepest valleys found within the specified measurement distance.  $R_a$  denotes the mean value obtained by calculating the absolute heights of the surface profile and taking their arithmetic average over the specified measurement distance. Rough copper foam has higher values of inherent roughness than the smooth substrate. Figure 1e,f depict SEM images of the copper foams used. The inherent roughness plays a crucial role in the shape of developed structures. Tree-like silver dendrites and flower-like structures grow on rougher copper foams, while nanowire morphologies and moss-like Ag dendrites are commonly found at smoother samples (see Figure 2).

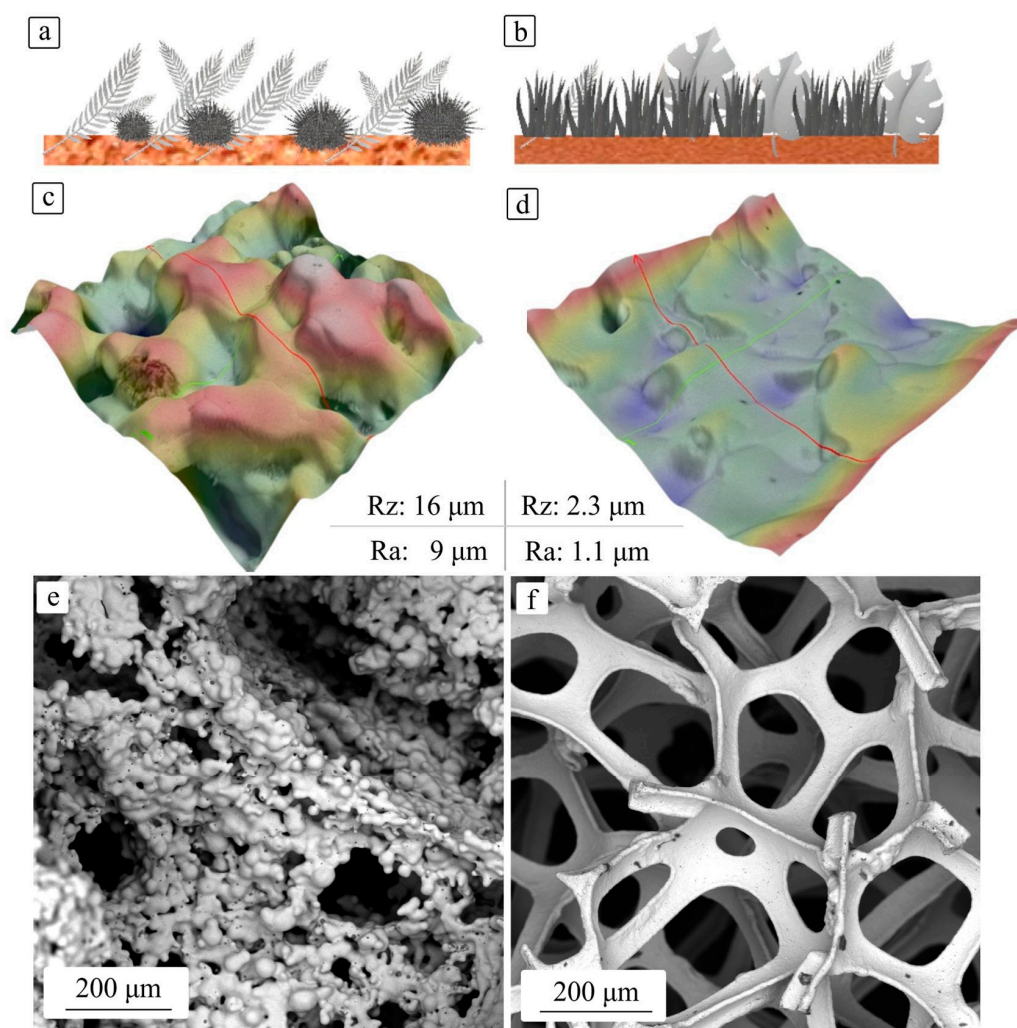


**Figure 1.** Schematic illustration of developed morphologies (a) on rough copper foam and (b) on smooth copper foam. Strut roughness of (c) rough copper foam and (d) smooth copper foam. SEM images of (e) rough copper foam and (f) smooth copper foam.

The emergence of Ag dendrites can be elucidated through a straightforward reaction mechanism. In this galvanic reaction, the reduction reaction  $\text{Ag}^+ + \text{e}^- = \text{Ag}$  occurs exclusively on the metal surface, initially on copper (Cu) and subsequently on the newly formed silver (Ag) [44]. The necessary electrons are supplied with the oxidation reaction  $\text{Cu} = \text{Cu}^{2+} + 2\text{e}^-$ , which takes place on the Cu surface, leading to the release of  $\text{Cu}^{2+}$  ions into the solution. Electron transport within the metal enables the reduction of  $\text{Ag}^+$  ions on the Ag surface. The spontaneous reduction of silver ions using copper can be described with the following reaction:  $2\text{Ag}^+ + \text{Cu} \rightarrow 2\text{Ag} + \text{Cu}^{2+}$  [45]. By immersing copper substrates in a silver nitrate solution, a series of thin silver films were deposited onto the substrates. Due to the minimal roughness of smooth copper foam, the reaction occurs at a slow pace, resulting in the formation of tiny voids within the film that are nearly imperceptible. However, when the roughness of the strut increases (rough copper foam), the reaction accelerates, leading to the emergence of larger fractal-like silver structures. As a result, the size of the voids between these structures also expands. (See Figure 1a,b).

The formation of silver dendrites has been the subject of extensive research studies. Silver dendrites are known for their ability to generate extensive specific surface areas [46]. Dendrite growth can be understood through various models, including deposition, diffusion and aggregation (DDA); diffusion-limited aggregation (DLA); oriented attachment (OA); and cluster–cluster aggregation (CCA) [47]. The anisotropic crystal growth of den-

rites occurs when kinetic factors dominate over thermodynamic factors, resulting in a non-equilibrium condition. The diffusion-limited aggregation model describes the fortuitous aggregation and asymmetric growth of nanoparticles, leading to the formation of fractal structures when the growth rate is limited by the diffusion rate of solute atoms (also known as random walkers) to the reaction interface [48]. Conversely, oriented attachment involves the spontaneous self-assembly and alignment of adjacent particles, resulting in a shared crystallographic orientation and the joining of these particles at a planar interface. The Cluster–Cluster Agglomeration (CCA) model, a dynamic cluster model, utilizes random motions to generate larger clusters by repeating the diffusion-limited aggregation (DLA) process [49].

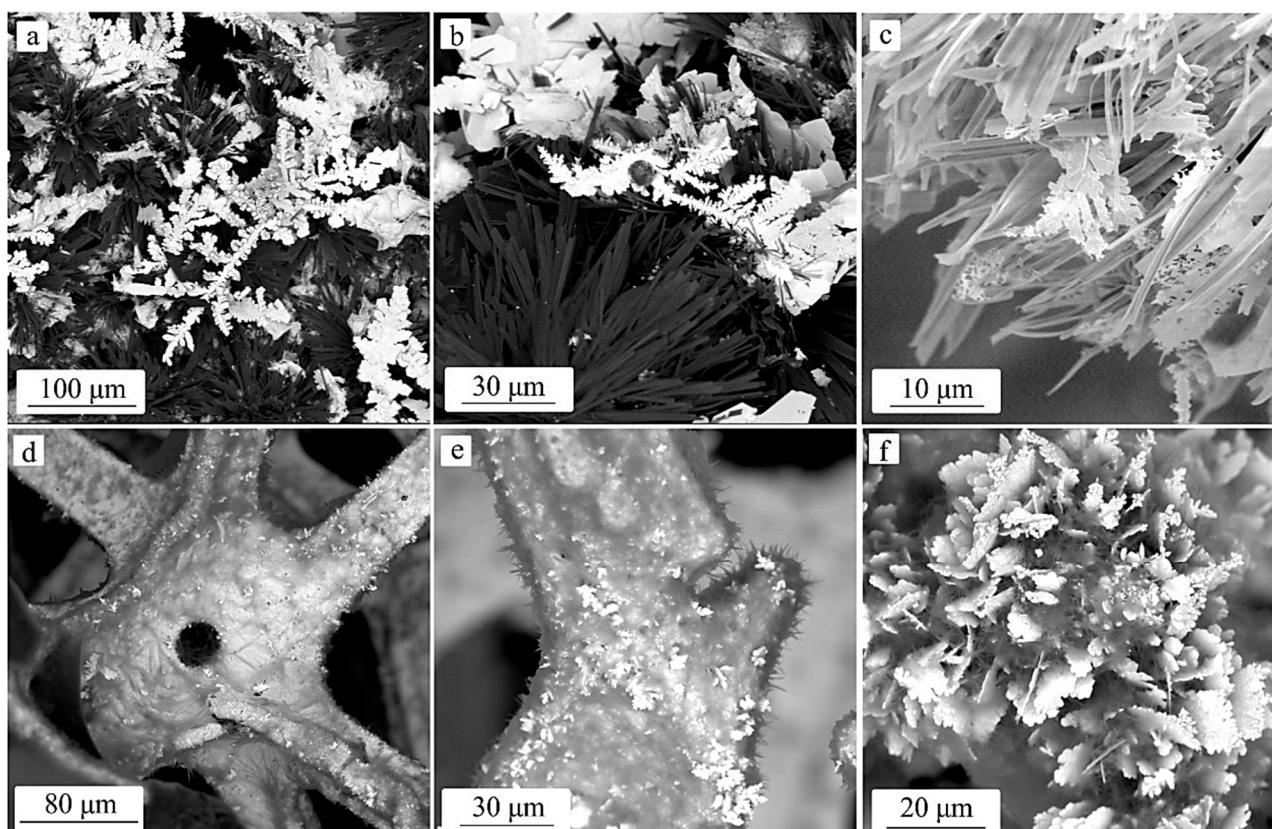


**Figure 2.** SEM images of superhydrophobic coating developed at 20 min immersion time in  $\text{AgNO}_3$  and 50 min in stearic acid solution, on rough copper foam (a–c), and on smooth copper foam (d–f).

In general, a fully formed main structure characterizes the dendritic silver nanostructure, showcasing distinct branches, stems and leaves. Certain secondary branches of the dendrites steadily extend and evolve into fresh trunks. These dendrite formations possessing such a shape are referred to as secondary branch structures. It is important to note that explaining the formation of Ag dendrites by considering only one of these mechanisms oversimplifies the actual phenomena. Therefore, it is common to invoke multiple mechanisms simultaneously to better understand the growth process of Ag dendrites [50].

Dendritic fractals can have one, two or multiple branches, extending from worm-like structures as primary dendrite arms as schematically shown in Figure 3. In the case of silver, the slightly elongated structures act as primary dendrite arms, serving as a central trunk for the growth of secondary dendritic structures through branching [51]. The transformation from branched structures to dendritic structures in silver is facilitated with the continuous supply of a new portion of the  $\text{AgNO}_3$  solution to the surface of the primary dendrite arm [52].

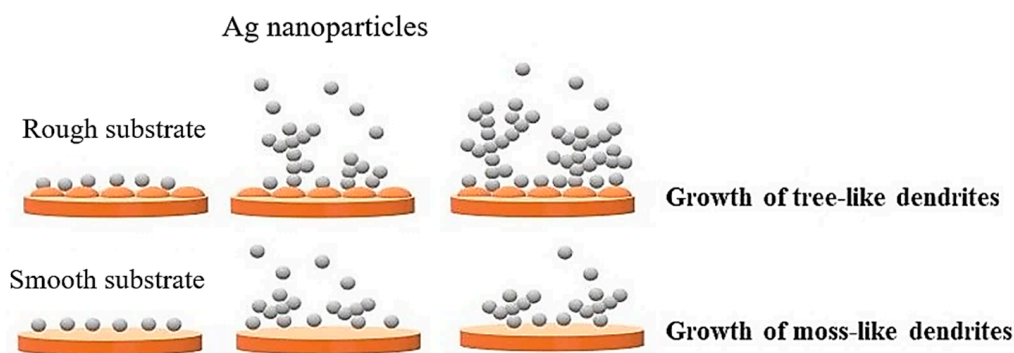


**Figure 3.** Schematic illustration of dendrites' growing mechanism on rough substrate and smooth substrate.

As the reaction time progresses, the concentration of silver ions diminishes, leading to a gradual reduction in the length of symmetrically shaped dendrites. Moreover, the dendrite structure undergoes degeneration, transitioning into a higher-order branched structure and the gaps between dendrites become narrower [43,53].

In the case of multilayer films of stearic acid, it is generally accepted that the first monolayer forms a chemical bond with the surface, while subsequent monolayers stack on top. A fatty acid becomes complexed with the surface metal atoms and forms the first monolayer alongside neighboring molecules [54–57]. The ordered arrangement of long-chain organic amphiphiles in monolayers is usually created using two main techniques: the Langmuir–Blodgett (LB) deposition method or through the process of spontaneous adsorption from a solution, commonly known as self-assembly (SA). There is a great similarity between monolayers produced through the self-assembly (SA) method and those created using the Langmuir–Blodgett (LB) method [58–61]. The adsorption process of stearic acid onto the silver surface is highly energetically favorable, making it relatively effortless to form complete monolayers by simply bringing the silver substrate into contact with the acid solution [47,48].

### 3.2. Oil–Water Separation

The oil–water separation performance of superhydrophobic copper foams with a different substrate roughness was conducted at 25 °C in a small tank (Figure 4a) with a volume ratio of  $V_{\text{oil}}:V_{\text{water}} = 1:3$ . Nine different types of oil with different viscosities (Figure 4b) were used. Separation efficiency was maintained above 94% after 10 cycles of filtration (Figure 4c). The significance of viscosity lies in its influence on the separation efficiency and absorption capacity of superhydrophobic copper foams. The efficiency of separating high viscous oils is lower compared to less viscous oils, whereas this fact is not observed in terms of absorption (Figure 4d). All pollutants have lower density than water. The findings from the separation efficiency results, as depicted in Figure 4c, indicate that roughness holds little significance as a contributing factor, with the primary determinant of efficiency being the crucial role played by viscosity. Conversely, it should be noted that when it comes to absorption capacity, roughness is a determining factor. Figure 4d depicts the absorption capacity values of superhydrophobic copper foams with the smooth and rough substrate, respectively. Smooth copper foam displays significantly greater absorption values in contrast to the foam with the rough base. Due to the greater uniformity of the pores, it is able to maintain a satisfactory level of oil evenly over its entire surface, unlike foam with a rough substrate. Furthermore, the microstructure of the coating on the smooth foam exhibits greater uniformity, without sizable voids, consequently leading to improved retention of contaminants.

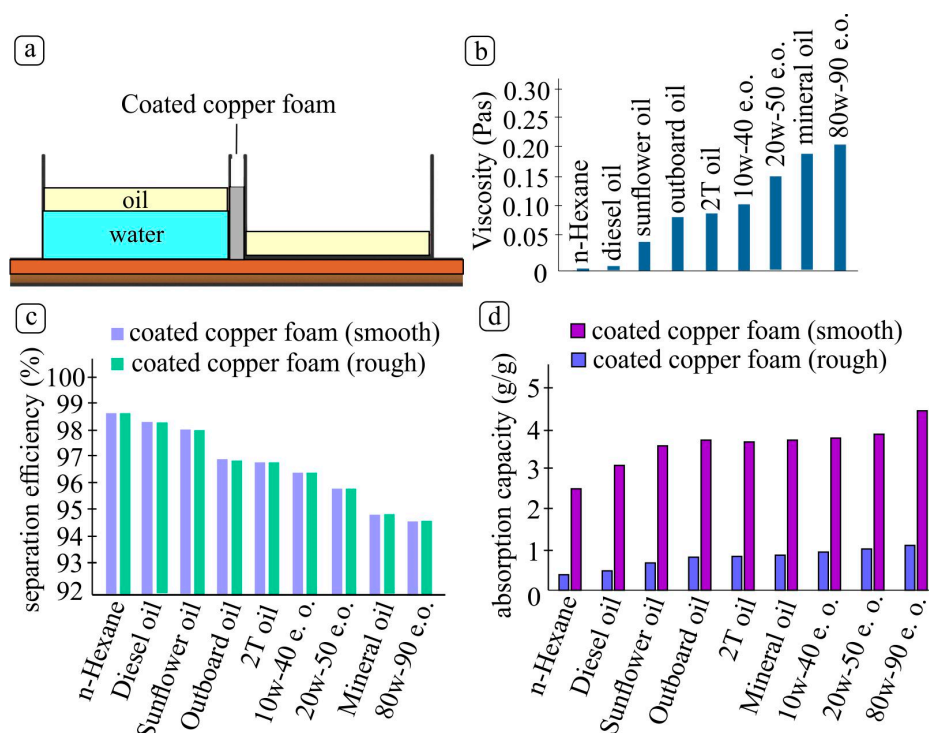


**Figure 4.** (a) Tank for oil–water separation, (b) oil viscosities used, (c) separation efficiency for different types of oil after 10 filtration cycles, (d) absorption capacity for various oils.

### 3.3. Thermal and Chemical Stability

To assess the environmental stability and durability of superhydrophobic copper foams, a comprehensive investigation was conducted to examine their response to exposure to different solutions and temperatures. Superhydrophobic copper foam samples were exposed to 100 °C in a laboratory incubator and to −15 °C in a cooling chamber, for 1, 4, 9, 16 and 40 h, respectively, in order to evaluate their stability under thermal conditions. Figure 5a illustrates WCA measurements for rough and smooth copper foam, taken after thermal loads, and the results show that their hydrophobic properties were maintained. It is noteworthy that in the smooth foam, the WCA values remain consistently high at around 140°, even after 40 h of exposure at both temperatures (100 °C and −15 °C), while the rough foam's contact angle decreased to 120° at 100 °C and 110° at −15 °C, after the same duration. Chemical stability of superhydrophobic copper foams was evaluated in acidic and alkaline solutions. The foam samples were immersed in HCl and NaOH solutions for 1, 4, 9, 16 and 40 h, correspondingly. Figure 5b illustrates the WCA values obtained after subjecting the samples to these chemical treatments. There is a consistent stabilization of the contact angle observed in both acidic and alkaline environments for both foams. Nonetheless, it is worth noting that the contact angles are notably higher in the foam with the smooth substrate. All the foams maintain their hydrophobic properties, even after 40 h of immersion.

Figure 6a–d depict the morphology of superhydrophobic smooth copper foams, after 40 h of exposure at 100 °C and −15 °C. Nanowire morphologies of stearic acid create aggregates, a fact that leads to an uneven distribution of the structure across the surface, and the leaf-like structure has undergone partial degradation. SEM images of the modified foams' morphologies following 40 h in the HCl and NaOH solutions are presented in Figure 6e–h. Regarding the morphologies when exposed to the acidic solution (Figure 6e,f), an extensive structural degradation was observed. Initial morphology of the coating's components was disrupted, leading to the formation of aggregates. Copper foam remains superhydrophobic as the substrate remains coated and no exfoliation of the coating was noted. Submerging the coated foam in an alkaline solution has a minor impact on its



morphology, but WCA reduction is probably due to the decrease in the quantity of its constituents on the foam substrate (Figure 6g,h).

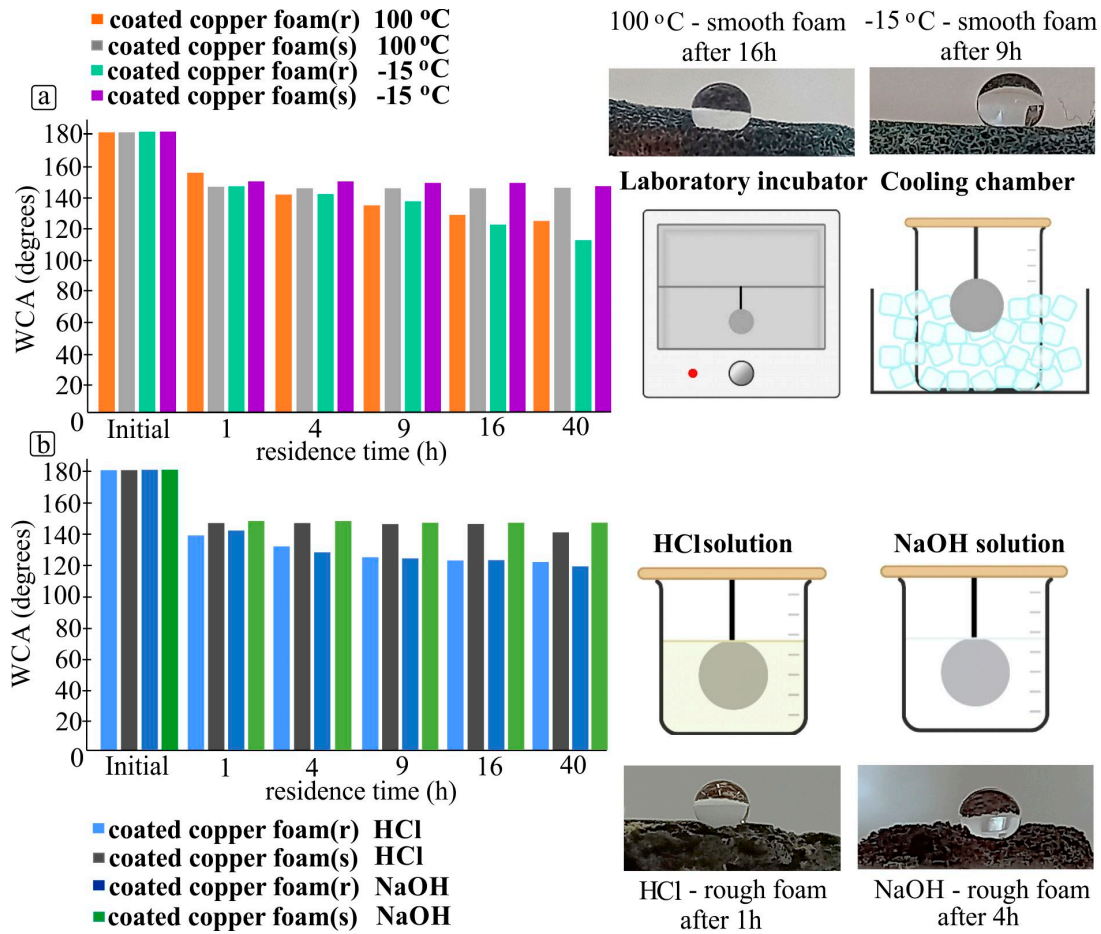


Figure 5. Contact angle measurements and indicative water droplet pictures (a) after thermal treatment at 100 °C and −15 °C and (b) after chemical treatment in HCl and NaOH solutions.

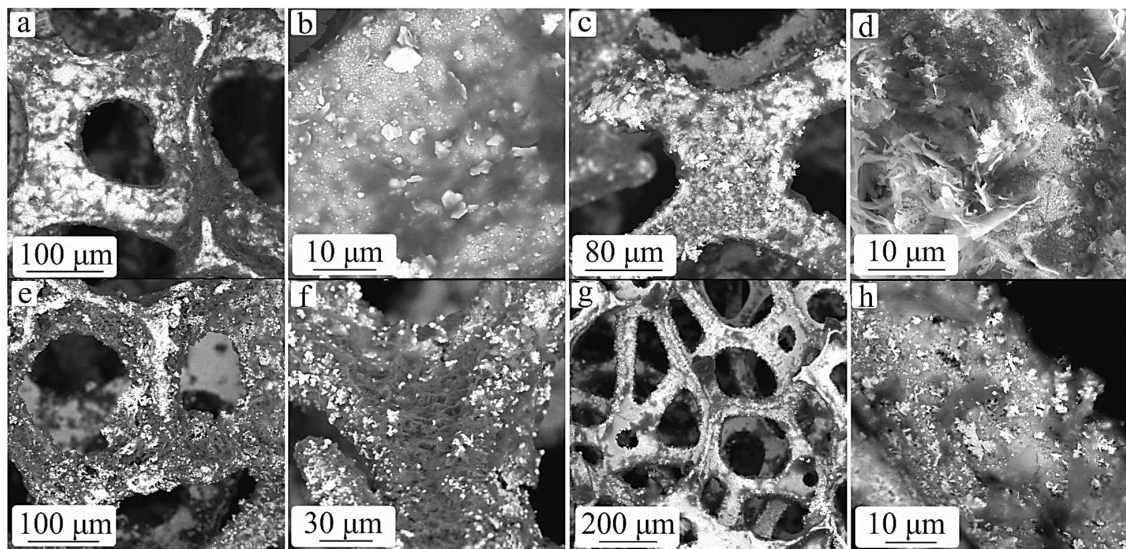
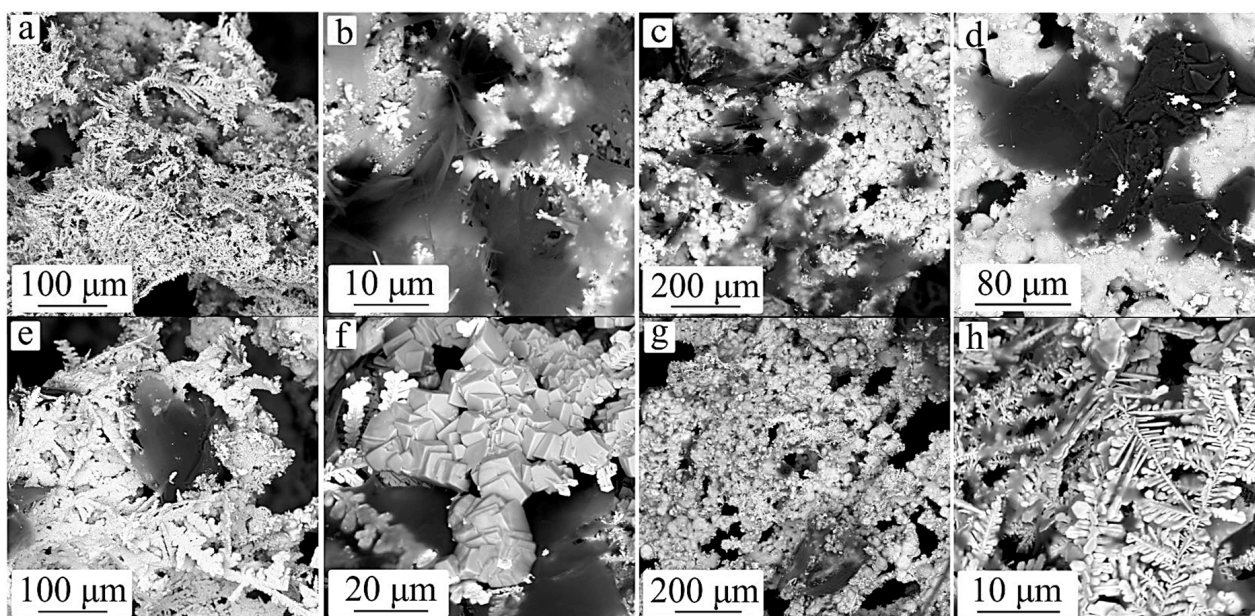


Figure 6. SEM images of smooth superhydrophobic copper foams, (a,b) after thermal treatment at 100 °C and (c,d) at −15 °C, and (e,f) after chemical treatment in HCl and (g,h) NaOH solutions, for 40 h.

Figure 7a,b illustrate the coating's structures on rough copper foam, after exposure for 40 h at 100 °C. Tree-like silver dendrites appear to have undergone slight melting and consolidation, while micro-flowers' petals undergo partial destruction and form aggregates. Regarding the exposure of the sample to −15 °C for 40 h (Figure 7c,d), there is a destruction as well as a detachment of dendritic morphologies and an extended degradation of micro-clusters. Dendritic branches separated from the stems and fused together, while micro-flowers were detached and completely lost their initial shape, after 40 h of residence in the HCl solution (Figure 7e,f). Figure 7g,h show both structures after 40 h of residence in the NaOH solution. The dendritic structures have undergone fragmentation in some places and aggregation in others, whilst micro-clusters have been thoroughly demolished and dispersed across different locations on the foam.



**Figure 7.** SEM images of rough superhydrophobic copper foams, (a,b) after thermal treatment at 100 °C and (c,d) at −15 °C, and after chemical treatment in (e,f) HCl solutions and (g,h) NaOH solutions, for 40 h.

### 3.4. Stability in Water and Sodium Chloride Solutions

To assess the viability of utilizing superhydrophobic foams for water purification applications involving the removal of pollutants such as oils, a comprehensive examination of their stability in water and the sodium chloride solution (3.5% *w/v*) was conducted. Figure 8a depicts copper foam's WCA measurements as a function of residence time in water and the sodium chloride solution. Both modified copper foams maintained their hydrophobic properties even after 40 h of immersion in both solutions. In comparison to immersion in water, the reduction in angle values is greater when the foams are submerged in the sodium chloride solution. During the initial hours of exposure, a decline in the angle is detected in both foams, whether they are immersed in water or a sodium chloride solution. Following approximately 10 h of immersion in the solutions, the angle in both foams reaches a stable state, maintaining a constant value even after 40 h in water and the NaCl solution. The foams retain their hydrophobic properties, as evidenced with the angle remaining close to 140°.

SEM images of silver-coated copper foams' morphologies after immersion in solutions for 40 h (Figure 8b–d) show that nanowire and dendritic structures on smooth copper foam have undergone reduction and partial degradation, while micro-flowers and tree-like morphologies on rough copper foam disintegrate and one structure adheres to another (Figure 8e–g). After exposure to the sodium chloride solution, deposits from the NaCl

components are observed on the foam (Figure 8h–j). Figure 8k–m depict that silver dendrites broken down into small particles and micro-flowers altered in shape from their original state.

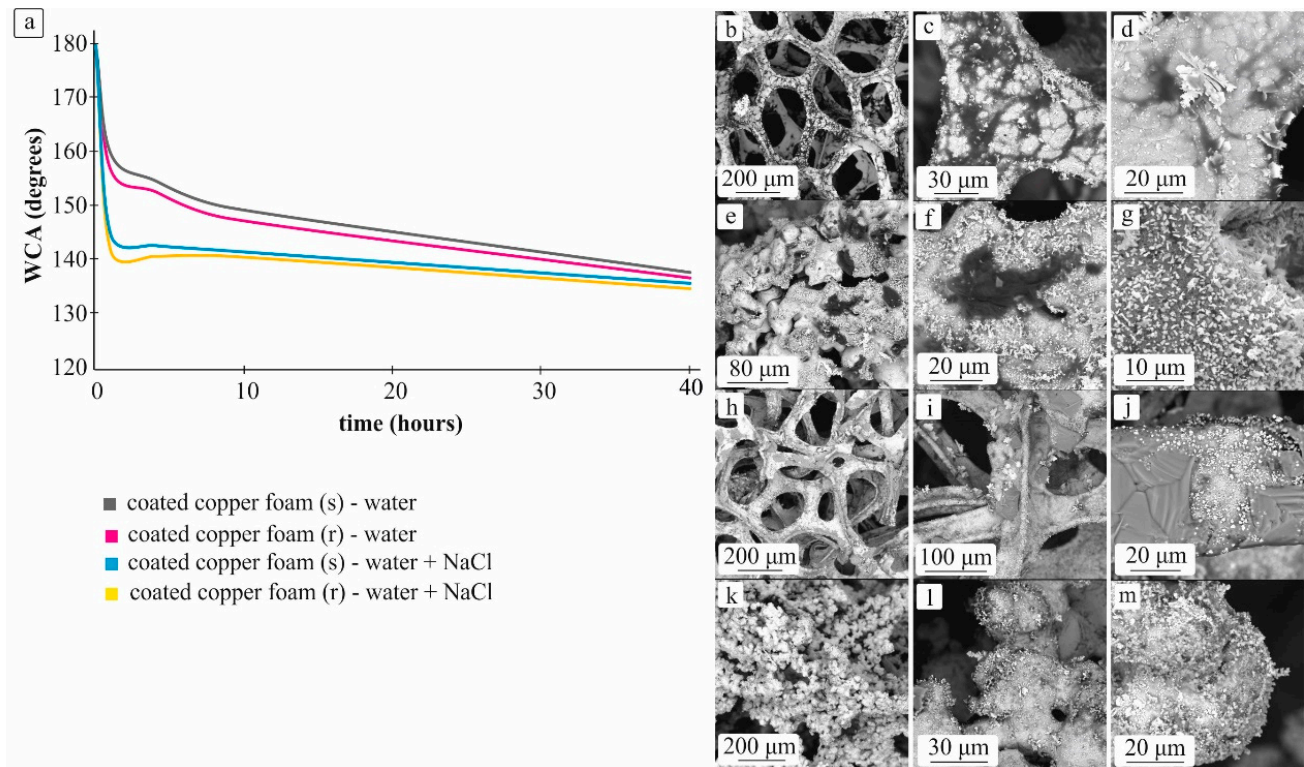


**Figure 8.** (a) Contact angle measurements after immersion in water and sodium chloride solution (SEM images of coated copper foams), (b–d) (smooth) after immersed in water, (e–g) (rough) after immersed in water, (h–j) (smooth) after immersed in sodium chloride solution, (k–m) (rough) after immersed in sodium chloride solution, for 40 h.

### 3.5. Mechanical Durability

Abrasion tests were carried out to evaluate the mechanical durability of the modified copper foams. Superhydrophobic copper foams were placed on a 600-grit SiC paper, using weights of 35 gr and 90 gr, and measurements of WCA were performed during multiple cycles of abrasion of a 20 cm length each (Figure 9a). After five cycles, a significant decrease in the contact angle is noted, but in the subsequent cycles, there is a substantial stabilization. This stability persists, maintaining the hydrophobicity in both foams for 35 gr and 90 gr. Hence, the substrate's surface roughness does not impact the mechanical stability of the coating during this test. Even after 40 cycles of abrasion, the samples maintained their hydrophobic properties. The weights applied are significantly larger in comparison to the weights of the foams, which amount to 0.2 gr for the rough foam and 0.07 gr for the smooth foam. It is evident that, for instance, 90 gr is 1285 times greater than the weight of the smooth foam. Consequently, both samples exhibit exceptional mechanical stability.

The stability of the superhydrophobic foams was also investigated using an ultrasonic device. The samples were positioned in the apparatus for various time durations. Samples exhibited hydrophobicity even after 90 min (Figure 9b). The foam with the smooth substrate exhibits slightly higher WCA values, demonstrating enhanced coating stability, due to the coating's uniformity.

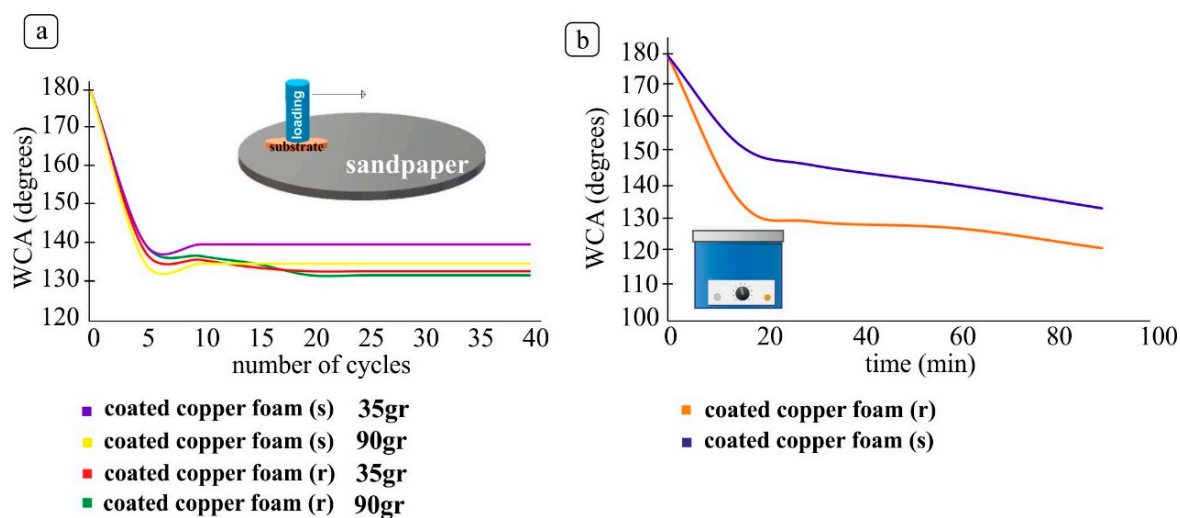


**Figure 9.** Contact angle measurements (a) after several cycles of abrasion on SiC paper with several weights on modified copper foams and (b) after various time durations of treatment in ultrasonic device.

#### 4. Conclusions

A superhydrophobic coating was effectively developed on copper foams with different levels of roughness by immersing them in  $\text{AgNO}_3$  and stearic acid solutions. The goal was to attain a long-lasting superhydrophobic copper foam featuring a water contact angle of 180 degrees, coupled with outstanding chemical and thermal resilience, as well as superior separation capability. Due to this fact, roughness of the substrate was evaluated with respect to the foam properties. The following conclusions can be drawn:

- (1) As the strut's roughness increases, stearic acid's nanosheets and self-assembled Ag clusters grow larger in size and length. Particularly, the stearic acid nanosheets form and start to vertically expand, resembling chrysanthemum petals.
- (2) The modified copper foams exhibited significant chemical and thermal stability. Specifically, WCA of the foam with the smooth substrate consistently stays high at approximately  $140^\circ$  even after 40 h of exposure at both temperatures ( $100^\circ\text{C}$  and  $-15^\circ\text{C}$ ). In contrast, after the same time duration, the contact angle of the foam having a rough substrate decreases to  $120^\circ$  at  $100^\circ\text{C}$  and  $110^\circ$  at  $-15^\circ\text{C}$ . A stable contact angle is consistently observed in both acidic and alkaline environments for both types of foams. However, contact angles for the samples with the smooth substrate have greater values. All the foams retain their hydrophobic characteristics, even following a 40 h immersion.
- (3) Mechanical durability of modified copper foams was tested with dragging and in ultrasounds, exhibiting outstanding results. The samples with the smooth substrate show higher WCA values, indicating improved coating stability attributed to the uniformity of the coating.
- (4) The separation efficiency of both foams remained above 94% for pollutants with several viscosities, indicating excellent stability and durability. Regarding absorption, the foam with the smooth substrate proved to be more efficient, retaining larger quantities of pollutants. The uniform porosity and coating's microstructure lacking significant voids leads to retaining the oil across its entire surface, a fact that improves its ability to retain contaminants.

**Author Contributions:** Conceptualization, F.S.; Methodology, A.B.; Validation, A.B.; Formal analysis, A.B.; Investigation, A.B.; Resources, F.S.; Data curation, A.B.; Writing—original draft, A.B.; Writing—review & editing, Visualization, A.B. and F.S.; Supervision, F.S.; Project administration, S.S. Funding acquisition, S.S. All authors have read and agreed to the published version of the manuscript.

**Funding:** This research was funded by the Research Committee, Aristotle University of Thessaloniki, grand number 89251.

**Institutional Review Board Statement:** Not applicable.

**Informed Consent Statement:** Not applicable.

**Data Availability Statement:** Data is contained within the article.

**Conflicts of Interest:** The authors declare no conflict of interest.

## References

1. Chanwoo, P.; Taegun, K.; Yong, K.; Min, W.L.; Seongpil, A.; Sam, Y. Supersonically sprayed transparent flexible multifunctional composites for self-cleaning, anti-icing, anti-fogging, and anti-bacterial applications. *Compos. B* **2021**, *222*, 109070.
2. Yuxing, B.; Haiping, Z.; Yuanyuan, S.; Hui, Z.; Jesse, Z. Recent Progresses of Superhydrophobic Coatings in Different Application Fields: An Overview. *Coatings* **2021**, *11*, 116.
3. Darband, G.B.; Aliofkhaei, M.; Khorsand, S.; Sokhanvar, S.; Kaboli, A. Science and Engineering of Superhydrophobic Surfaces: Review of Corrosion Resistance, Chemical and Mechanical Stability. *Arab. J. Chem.* **2020**, *13*, 1763–1802. [[CrossRef](#)]
4. Rasouli, S.; Rezaei, N.; Hamed, H.; Zendejboudi, S.; Duan, X. Superhydrophobic and superoleophilic membranes for oil-water separation application: A comprehensive review. *Mater. Des.* **2021**, *204*, 109599. [[CrossRef](#)]
5. Bhushan, B. Bioinspired oil–water separation approaches for oil spill clean-up and water purification. *Philos. Trans.* **2019**, *377*, 20190120. [[CrossRef](#)] [[PubMed](#)]
6. Gupta, R.K.; Dunderdale, G.J.; England, M.W.; Hozumi, A. Oil/water separation techniques: A review of recent progresses and future directions. *J. Mater. Chem.* **2017**, *5*, 16025–16058. [[CrossRef](#)]
7. Yue, H.; Yanji, Z.; Huaiyuan, W.; Chijia, W.; Hongwei, L.; Xiguang, Z.; Ruixia, Y.; Yiming, Z. Facile preparation of superhydrophobic metal foam for durable and high efficient continuous oil-water separation. *J. Chem. Eng.* **2017**, *322*, 157–166.
8. Yangyang, C.; Shengke, Y.; Qian, Z.; Dan, Z.; Chunyan, Y.; Zongzhou, W.; Runze, W.; Rong, S.; Wenke, W.; Yaqian, Z. Effects of Surface Microstructures on Superhydrophobic Properties and Oil-Water Separation Efficiency. *Coatings* **2019**, *9*, 69.
9. Collins, C.M.; Safiuddin, M. Lotus-Leaf-Inspired Biomimetic Coatings: Different Types, Key Properties, and Applications in Infrastructures. *Infrastructures* **2022**, *7*, 46. [[CrossRef](#)]
10. Ensikat, H.J.; Ditsche-Kuru, P.; Neinhuis, C.; Barthlott, W. Superhydrophobicity in perfection: The outstanding properties of the lotus leaf. *Beilstein J. Nanotechnol.* **2011**, *2*, 152–161. [[CrossRef](#)]
11. Parvate, S.; Chattopadhyay, S. Complex Polymeric Microstructures with Programmable Architecture via Pickering Emulsion-Templated In Situ Polymerization. *Langmuir* **2022**, *38*, 1406–1421. [[CrossRef](#)]
12. Mengru, J.; Qianli, X.; Zikang, C. A Review: Natural Superhydrophobic Surfaces and Applications. *J. Biomater. Nanobiotechnol.* **2020**, *11*, 110–149.
13. Aguilar-Morales, A.I.; Alamri, S.; Voisiat, B.; Kunze, T.; Lasagni, A.F. The Role of the Surface Nano-Roughness on the Wettability Performance of Microstructured Metallic Surface Using Direct Laser Interference Patterning. *Materials* **2019**, *12*, 2737. [[CrossRef](#)]
14. Goswami, A.; Pillai, S.C.; McGranaghan, G. Surface modifications to enhance dropwise condensation. *Surf. Interfaces* **2021**, *5*, 101143. [[CrossRef](#)]
15. Dingliang, D.; Jianhao, Q.; Lu, Z.; Hong, M.; Jianfeng, Y. Amino-functionalized Ti-metal-organic framework decorated BiOI sphere for simultaneous elimination of Cr(VI) and tetracycline. *J. Colloid Interface Sci.* **2022**, *607*, 933–941.
16. Tao, L.; Hebin, L.; Wenxuan, C.; Yankang, D.; Qingli, Q.; Wenjing, M.; Ranhua, X.; Chaobo, H. Blow-spun nanofibrous composite Self-cleaning membrane for enhanced purification of oily wastewater. *J. Colloid Interface Sci.* **2022**, *608*, 2860–2869.
17. Nia, L.; Zhua, C.; Zhanga, S.; Caia, P.; Airoudj, A.; Vonna, L.; Hajjar-Garreaub, S.; Chemtob, A. Light-induced crystallization-driven formation of hierarchically ordered superhydrophobic sol-gel coatings. *Prog. Org. Coat.* **2019**, *135*, 255–262. [[CrossRef](#)]
18. Yu, Z.; Zhentao, Z.; Junling, Y.; Yunkai, Y.; Huafu, Z. A Review of Recent Advances in Superhydrophobic Surfaces and Their Applications in Drag Reduction and Heat Transfer. *Nanomaterials* **2022**, *12*, 44. [[CrossRef](#)]
19. Sotoudeh; Mousavi, S.M.; Karimi, N.; Lee, B.J.; Abolfazli-Esfahani, J.; Manshadi, M.K.D. Natural and synthetic superhydrophobic surfaces: A review of the fundamentals, structures, and applications. *Alex. Eng. J.* **2023**, *68*, 587–609. [[CrossRef](#)]
20. Shuangshuang, X.; Qing, W.; Ning, W. Chemical Fabrication Strategies for Achieving Bioinspired Superhydrophobic Surfaces with Micro and Nanostructures: A Review. *Adv. Eng. Mater.* **2021**, *23*, 2001083.
21. Avramescu, R.E.; Ghica, M.V.; Dinu-Pîrvu, C.; Prisada, R.; Popa, L. Superhydrophobic Natural and Artificial Surfaces—A Structural Approach. *Materials* **2018**, *11*, 866. [[CrossRef](#)] [[PubMed](#)]
22. Liping, D.; Meng, C.; Huiying, L.; Haochen, H.; Xia, L.; Yanqing, W. 3D multiscale sponges with plant-inspired controllable superhydrophobic coating for oil spill cleanup. *Prog. Org. Coat.* **2021**, *151*, 106075. [[CrossRef](#)]
23. Yihao, G.; Fangqin, C.; Zihai, P. Superwetting Polymeric Three Dimensional (3D) Porous Materials for Oil/Water Separation: A Review. *Polymers* **2019**, *11*, 806. [[CrossRef](#)]
24. Tao, L.; Hebin, L.; Wenxuan, C.; Yankang, D.; Qingli, Q.; Wenjing, M.; Ranhua, X.; Chaobo, H. Blow-Spun Nanofibrous Membrane for Simultaneous Treatment of Emulsified Oil/Water Mixtures, Dyes, and Bacteria. *Langmuir* **2022**, *38*, 15729–15739.

25. Guoqiang, X.; Congyi, W.; Weinan, L.; Miaozheng, W.; Yu, H.; Youmin, R. Fabrication of super-wetting copper foam based on laser ablation for selective and efficient oil-water separation. *Surf. Coat. Technol.* **2021**, *424*, 127650.
26. Wanqing, Z.; Shaohua, W.; Wenlong, T.; Kang, H.; Cheng-xing, C.; Yalei, Z.; Yuping, Z.; Zheng, W.; Shouren, Z.; Lingbo, Q. Fabrication of a superhydrophobic surface using a simple in situ growth method of HKUST-1/copper foam with hexadecanethiol modification. *New J. Chem.* **2020**, *44*, 7065.
27. Song, Y.; Liu, Y.; Zhan, B.; Kaya, C.; Stegmaier, T.; Han, Z.; Ren, L. Fabrication of Bioinspired Structured Superhydrophobic and Superoleophilic Copper Mesh for Efficient Oil-water Separation. *J. Bionic Eng.* **2017**, *14*, 497–505. [[CrossRef](#)]
28. Yu-Ping, Z.; Jing-Hua, Y.; Ling-Li, L.; Cheng-Xing, C.; Ying, L.; Shan-Qin, L.; Xiao-Mao, Z.; Ling-Bo, Q. Facile Fabrication of Superhydrophobic Copper-Foam and Electrospinning Polystyrene Fiber for Combinational Oil–Water Separation. *Polymers* **2019**, *11*, 97. [[CrossRef](#)]
29. Jia, X.; Jinliang, X.; Yang, C.; Xianbing, J.; Yuying, Y. Fabrication of non-flaking, superhydrophobic surfaces using a one-step solution-immersion process on copper foams. *Appl. Surf. Sci.* **2013**, *286*, 220–227. [[CrossRef](#)]
30. Wei, Z.; Guangji, L.; Liying, W.; Zhifeng, C.; Yinlei, L. A facile method for the fabrication of a superhydrophobic polydopamine-coated copper foam for oil/water separation. *Appl. Surf. Sci.* **2017**, *413*, 140–148.
31. Zehao, C.; Jihao, Z.; Ting, Z.; Qing, T.; Yunjun, N.; Shouping, X.; Jiang, C.; Xiufang, W.; Pihui, P. Superhydrophobic copper foam bed with extended permeation channels for water-in-oil emulsion separation with high efficiency and flux. *J. Environ. Chem. Eng.* **2023**, *11*, 109018. [[CrossRef](#)]
32. Ruixi, G.; Xiang, L.; Tian, C.Z.; Like, Q.; Ying, L.; Shaojun, Y. Superhydrophobic Copper Foam Modified with n-Dodecyl Mercaptan-CeO<sub>2</sub> Nanosheets for Efficient Oil/Water Separation and Oil Spill Cleanup. *Ind. Eng. Chem. Res.* **2020**, *59*, 21510–21521.
33. Ji, L.; Ruixi, G.; Yuan, W.; Tian, C.Z.; Shaojun, Y. Superhydrophobic palmitic acid modified Cu(OH)<sub>2</sub>/CuS nanocomposite-coated copper foam for efficient separation of oily wastewater. *Colloids Surf. A Physicochem. Eng.* **2022**, *637*, 128249. [[CrossRef](#)]
34. Haiyan, Z.; Lin, G.; Xinquan, Y.; Caihua, L.; Youfa, Z. Durability evaluation of superhydrophobic copper foams for long-term oil-water separation. *Appl. Surf. Sci.* **2017**, *407*, 145–155. [[CrossRef](#)]
35. Jian, R.; Tao, Z.; Fengxian, Q.; Jicheng, X.; Yao, Z.; Dongya, Y.; Yuting, D. Design and preparation of efficient, stable and superhydrophobic copper foam membrane for selective oil absorption and consecutive oil–water separation. *Mater. Des.* **2018**, *142*, 83–92. [[CrossRef](#)]
36. Haiyan, Z.; Doudou, L.; Mingjuan, C.; Xinquan, Y.; Youfa, Z. Sprayed superamphiphilic copper foams for long term recoverable oil-water separation. *Surf. Coat. Technol.* **2018**, *334*, 394–401. [[CrossRef](#)]
37. Chunhua, L.; Yun, P.; Conglin, H.; Yuzhen, N.; Jiaoping, S.; Yibao, L. Bioinspired Superhydrophobic/Superhydrophilic Janus Copper Foam for On-Demand Oil/Water Separation. *ACS Appl. Mater. Interfaces* **2022**, *14*, 11981–11988.
38. Baxevani, A.; Stergioudi, F.; Patsatzis, N.; Malletzidou, L.; Vourlias, G.; Skolianos, S. Preparation and Characterization of Stable Superhydrophobic Copper Foams Suitable for Treatment of Oily Wastewater. *Coatings* **2023**, *13*, 355. [[CrossRef](#)]
39. Stergioudi, F.; Baxevani, A.; Mavropoulos, A.; Skordaris, G. Deposition of Super-Hydrophobic Silver Film on Copper Substrate and Evaluation of Its Corrosion Properties. *Coatings* **2021**, *11*, 1299. [[CrossRef](#)]
40. Xiulan, L.; Xiaohong, H.; Yao, L.; Zhongxiang, B.; Chenchen, L.; Xiaobo, L.; Kun, J. In-situ growth of silver nanoparticles on sulfonated polyarylene ether nitrile nanofibers as super-wetting antibacterial oil/water separation membranes. *J. Membr. Sci.* **2023**, *675*, 121539.
41. Dong, C.; Zhang, X.; Cai, H.; Cao, C.; Zhou, K.; Wang, X.; Xiao, X. Synthesis of stearic acid-stabilized silver nanoparticles in aqueous solution. *Adv. Powder Technol.* **2016**, *27*, 2416–2423. [[CrossRef](#)]
42. Liu, H.; Cheng, X.B.; Jin, Z.; Zhang, R.; Wang, G.; Chen, L.Q.; Liu, Q.B.; Huang, J.Q.; Zhang, Q. Recent advances in understanding dendrite growth on alkali metal anodes. *Energy Chem.* **2019**, *1*, 100003. [[CrossRef](#)]
43. Cai, W.F.; Pu, K.B.; Ma, Q.; Wang, Y.H. Insight into the fabrication and perspective of dendritic Ag nanostructures. *J. Exp. Nanosci.* **2017**, *12*, 319–337. [[CrossRef](#)]
44. Khaskhoussi, A.; Calabrese, L.; Patané, S.; Proverbio, E. Effect of Chemical Surface Texturing on the Superhydrophobic Behavior of Micro–Nano-Roughened AA6082 Surfaces. *Materials* **2021**, *14*, 7161. [[CrossRef](#)] [[PubMed](#)]
45. Yong, J.; Chen, F.; Yang, Q.; Huoa, J.; Hou, X. Superoleophobic surfaces. *Chem. Soc. Rev.* **2017**, *46*, 4113–4376. [[CrossRef](#)]
46. Safaee, A.; Sarkar, D.K.; Farzaneh, M. Superhydrophobic properties of silver-coated films on copper surface by galvanic exchange reaction. *Appl. Surf. Sci.* **2008**, *254*, 2493–2498. [[CrossRef](#)]
47. Bahadori, S.R.; Mei, L.; Athavale, A.; Chiu, Y.; Pickering, C.S.; Hao, Y. New Insight into Single-Crystal Silver Dendrite Formation and Growth Mechanisms. *Cryst. Growth Des.* **2020**, *20*, 7291–7299. [[CrossRef](#)]
48. Chen, R.; Nguyen, Q.N.; Xia, Y. Oriented Attachment: A Unique Mechanism for the Colloidal Synthesis of Metal Nanostructures. *ChemNanoMat* **2022**, *8*, e202100474. [[CrossRef](#)]
49. Chu, J.; Zhao, Y.; Li, S.H.; Li, W.W.; Chen, X.Y.; Huang, Y.X.; Chen, Y.P.; Qu, W.G.; Yu, H.Q.; Xu, A.W.; et al. A highly-ordered and uniform sunflower-like dendritic silver nanocomplex array as reproducible SERS substrate. *RSC Adv.* **2015**, *5*, 3860. [[CrossRef](#)]
50. Ge, D.; Yao, J.; Ding, J.; Babangida, A.A.; Zhu, C.; Ni, C.; Zhao, C.; Qian, P.; Zhang, L. Growth mechanism of silver dendrites on porous silicon by single-step electrochemical synthesis method. *Appl. Phys.* **2022**, *128*, 908. [[CrossRef](#)]
51. Boles, M.A.; Engel, M.; Talapin, D.V. Self-Assembly of Colloidal Nanocrystals: From Intricate Structures to Functional Materials. *Chem. Rev.* **2016**, *116*, 11220–11289. [[CrossRef](#)] [[PubMed](#)]

52. Dinga, H.P.; Xina, G.Q.; Chena, K.C.; Zhanga, M.; Liub, Q.; Haoa, J.; Liu, H.G. Silver dendritic nanostructures formed at the solid/liquid interface via electroless deposition. *Colloids Surf. A Physicochem. Eng.* **2010**, *353*, 166–171. [[CrossRef](#)]
53. Gawert, C.; Bähr, R. Automatic Determination of Secondary Dendrite Arm Spacing in AlSi-Cast Microstructures. *Materials* **2021**, *14*, 2827. [[CrossRef](#)]
54. Ahmed, I.; Haque, A.; Bhattacharyya, S.; Patra, P.; Plaisier, J.R.; Perissinotto, F.; Bal, J.K. Vitamin C/Stearic Acid Hybrid Monolayer Adsorption at Air-Water and Air-Solid Interfaces. *ACS Omega* **2018**, *3*, 15789–15798. [[CrossRef](#)] [[PubMed](#)]
55. Norazura, A.M.H.; Sivaruby, K.; Mat Dian, N.L.H. Blended palm fractions as confectionery fats: A preliminary study. *J. Oil Palm Res.* **2021**, *33*, 360–380. [[CrossRef](#)]
56. Xu, C.L.; Wang, Y.Z. Self-assembly of stearic acid into nano flowers induces the tunable surface wettability of polyimide film. *Mater. Des.* **2018**, *138*, 30–38. [[CrossRef](#)]
57. Chao, Y.; Yaoguang, W.; Hongyan, F.; Sainan, Y.; Yingming, Z.; Hairong, Y.; Wei, J.; Bin, L. A stable eco-friendly superhydrophobic/superoleophilic copper mesh fabricated by one-step immersion for efficient oil/water separation. *Surf. Coat. Technol.* **2019**, *359*, 108–116.
58. Bike, M.J.B.; Benessoubo, K.D.; Eko, M.C.; Tekoumbo, T.L.C.; Elimbi, A.; Kamga, R. Adsorption mechanisms of pigments and free fatty acids in the discoloration of shea butter and palm oil by an acid-activated Cameroonian smectite. *Sci. Afri.* **2020**, *9*, e00498.
59. Patti, A.; Lecocq, H.; Serghei, A.; Acierno, D.; Cassagnau, P. The universal usefulness of stearic acid as surface modifier: Applications to the polymer formulations and composite processing. *J. Ind. Eng. Chem.* **2021**, *96*, 1–33. [[CrossRef](#)]
60. Syed Arshad, H.; Bapi, D.; Bhattacharjee, D.; Mehta, N. Unique supramolecular assembly through Langmuir Blodgett (LB) technique. *Heliyon* **2018**, *4*, e01038. [[CrossRef](#)]
61. Swierczewski, M.; Bürgi, T. Langmuir and Langmuir–Blodgett Films of Gold and Silver Nanoparticles. *Langmuir* **2023**, *39*, 2135–2151. [[CrossRef](#)] [[PubMed](#)]

**Disclaimer/Publisher's Note:** The statements, opinions and data contained in all publications are solely those of the individual author(s) and contributor(s) and not of MDPI and/or the editor(s). MDPI and/or the editor(s) disclaim responsibility for any injury to people or property resulting from any ideas, methods, instructions or products referred to in the content.